Computational Study of Error-field Effects on W7-X Stellarator Equilibria

C. Nührenberg[1], A.H. Boozer[2]

[1] *IPP, EURATOM Association, Wendelsteinstr. 1, 17491 Greifswald, Germany*

[2] *Columbia University, New York NY 10027, USA*

1 Introduction

The Wendelstein 7-X (W7-X, [1]) stellarator currently under construction [2] in Greifswald, Germany, has been designed to operate in a low-shear rotational transform regime around unity, which is relatively free from low-order rationals. As an important part of the W7-X divertor concept, the main operation scenarios will have the $5/m$, $m = 4,5,6$ island chains inherent to the five-periodic stellarator in their respective plasma edge regions. With the presence or vicinity of the low-order rational $\iota = 1$, however, possible magnetic error fields can destroy the periodicity of the stellarator field and, thus, hamper plasma performance. The impact of error-fields on the W7-X high-ι variant with $\iota \approx 1$ near the magnetic axis and $\iota \approx 5/4$ near the plasma edge is studied here. As a first application, $m = 1$ field perturbations are considered which retain the five-fold periodicity of the plasma, but dislocate the magnetic axis. With the perturbed-equilibrium method [3], an approach alternative to standard equilibrium calculations, as done with VMEC [4] or PIES [5]), was developed to computationally assess the impact of such error fields on stellarator equilibria [6].

2 Perturbed Equilibria

This section gives a short summary of the concept of perturbed equilibria. A detailed description is found in Refs. [3, 6].

An initial or unperturbed plasma state is slightly perturbed which is defined by a set of magnetic surfaces and two profiles, the rotational transform ι and the pressure p. The ideal MHD equilibrium for the perturbed plasma state is $\nabla(p_0 + p_1) = (\vec{\jmath}_0 + \vec{\jmath}_1) \times (\vec{B}_0 + \vec{B}_1)$. Subscripts $0(1)$ refer to unperturbed (perturbed) quantities, e.g. the magnetic field $\vec{B}$ and the current density $\vec{\jmath}$. Then the stationarity of $\delta^1 W + \delta^2 W = \int (\nabla p_0 - \vec{\jmath}_0 \times \vec{B}_0) \cdot \vec{\xi}\, \mathrm{d}^3 r - \frac{1}{2} \int \vec{\xi} \cdot \mathscr{F}[\vec{\xi}] \mathrm{d}^3 r$ is needed for a perturbed equilibrium. It is given by $\mathscr{F}[\vec{\xi}] = \vec{g}$, where $\mathscr{F}$ is the ideal MHD force operator acting on the displacement $\vec{\xi}$. The right-hand-side $\vec{g}$ derives from the perturbed plasma force $\vec{\xi} \cdot (\nabla p_0 - \vec{\jmath}_0 \times \vec{B}_0)$ and is non-zero for a non-equilibrium unperturbed state. The perturbed-magnetic-field normal component

$$B_{1n} = \vec{B}_1 \cdot \vec{n} = \vec{n} \cdot \nabla \times (\vec{\xi} \times \vec{B}_0) \quad (1)$$

must be continuous across any interface. Here, $\vec{n} = \nabla s / |\nabla s|$ is the outer unit normal to a magnetic surface $s = \mathrm{const}$. The normalized toroidal flux is used as a flux label. Force balance

$$\left[p + \frac{1}{2} |\vec{B}|^2 \right]_{inside} = \left[p + \frac{1}{2} |\vec{B}|^2 \right]_{outside} \quad , \quad (2)$$

which must hold at any interface, and the continuity of B_{1n} are the boundary conditions for the perturbed-equilibrium calculation.

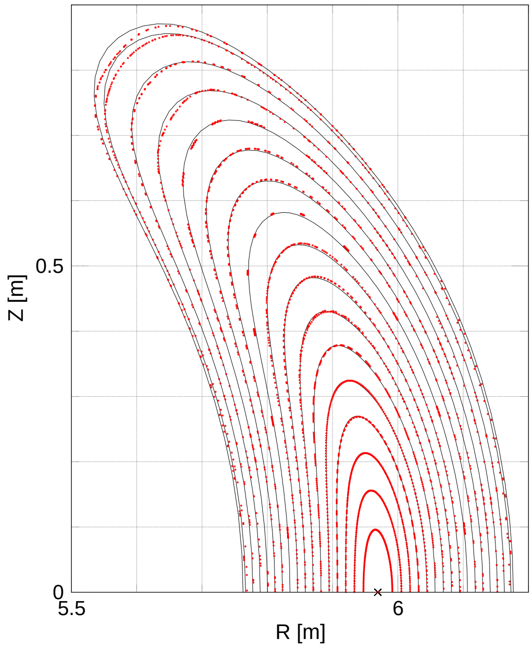

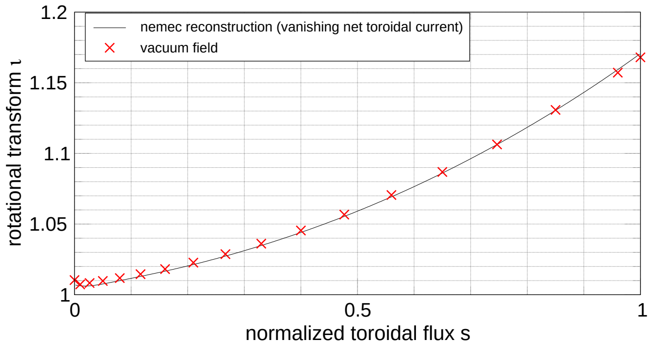

Figure 1: Top: Vacuum rotational transform of the high-ι W7-X variant: Comparison of the NEMEC reconstruction (black) and the vacuum magnetic field (red). Left: Top half of the bean-shaped cross-section of the high-ι W7-X variant: Comparison of the NEMEC reconstruction (black) and the vacuum magnetic field (red).

3 The W7-X high-ι variant

The W7-X high-ι configuration under the influence of an inward shift of the plasma column was chosen as a testbed for benchmarking the CAS3D perturbed-equilibrium calculation against the respective vacuum solution.

W7-X is a five-period device with ten identical half-modules. Its magnet system is built from three coil subsystems comprising fifty modular coils with five different coils per half-module (numbered 1, ..., 5 in Tab. 1), twenty planar coils with two different coils per half-module (labeled A and B), and ten identical control-saddle coils, one per half-module (label S). The planar or auxiliary coils provide flexibility in rotational transform; they carry no current in the W7-X standard case with $5/6 < \iota_{\text{vac}} < 5/5$; their current load needed for the W7-X high-ι case with $5/5 < \iota_{\text{vac}} < 5/4$ is given in Tab. 1. An inward shift of the plasma column is obtained by choosing slightly different currents in the auxiliary coils (see Tab. 1).

coil	1	2	3	4	5	A	B	S
high-ι	1.6	1.6	1.6	1.6	1.6	-0.352	-0.352	0
inward-shifted	1.6	1.6	1.6	1.6	1.6	-0.320	-0.384	0

Table 1: *W7-X magnet-system current loads [MA] for the two vacuum fields studied here.*

As shown in Fig. 1, the W7-X high-ι vacuum field was reconstructed to a good approximation by a zero-β run of the VMEC equilibrium code in its free-boundary version, i.e. the NEMEC code [4]. The toroidal flux enclosed by the outermost NEMEC surface was chosen to be $F_T = 1.7$ Vs. The left frame of Fig. 1 shows a comparison of the NEMEC flux surfaces (black) and the result of field-line tracing in the vacuum field. The NEMEC and vacuum field rotational transforms are given in the plot on the right. This zero-β NEMEC equilibrium is used as the basis for a CAS3D perturbed-equilibrium calculation. On its boundary the difference between the inward-shifted and the high-ι vacuum fields was sampled to find the normal component of the corresponding magnetic field perturbation B_{1n} of Eq. (1). Contours of the sampled B_{1n} are shown in the left frame

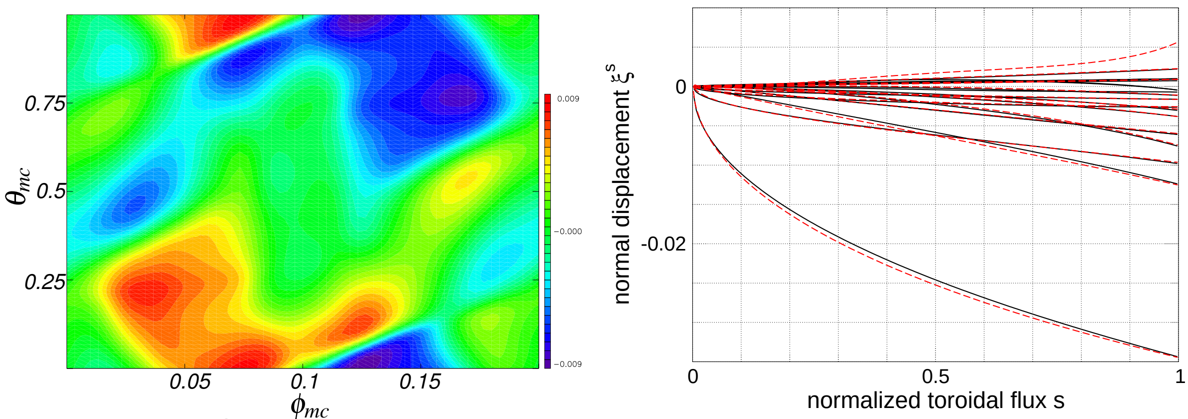

Figure 2: Left: Contours of the external B_{1n} on the plasma boundary; one field-period is shown with $\phi_{mc} = 0$ the bean-shaped, $\phi_{mc} = 0.1$ the triangular cross-section. $\theta_{mc} = 0$ is on the outside of the torus, $\theta_{mc} = 0.5$ at the inside. Regions near the maximum (minimum) of 0.009 T (-0.009 T) appear in red (blue). Right: Normal displacement harmonics describing the inward-shifted field. CAS3D (red) and NEMEC (black) results are compared.

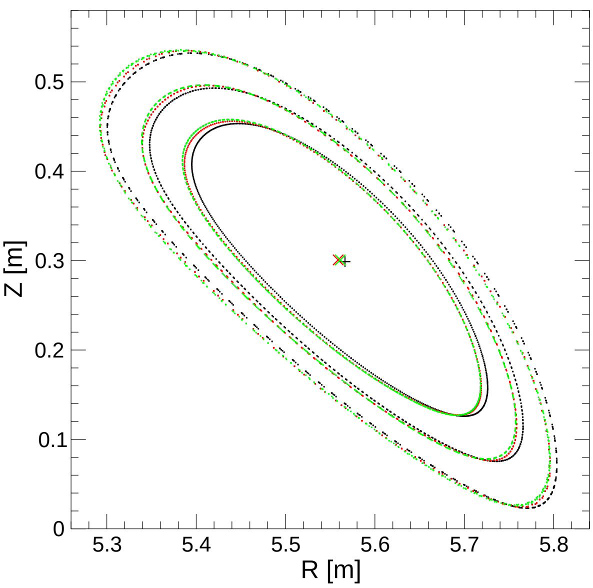

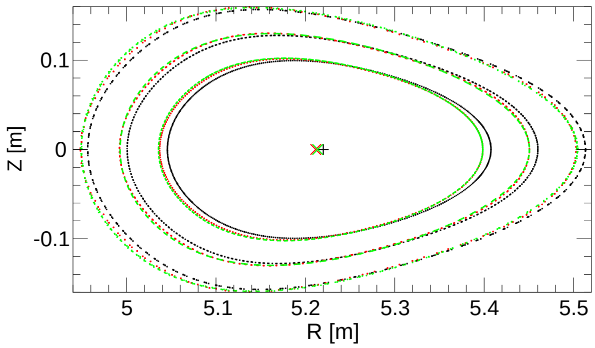

Figure 3: Left (top): Inward shift of the plasma column illustrated by the axis and three field-lines on the cross-section at a quarter (half) of a field period. The unperturbed (black) and perturbed (red) vacuum fields are compared with the perturbed field (green) resulting from CAS3D in its perturbed-equilibrium version.

of Fig. 2. One field-period is given with $\phi_{mc} = 0$ in the bean-shaped, $\phi_{mc} = 0.1$ in the triangular cross-section. $\theta_{mc} = 0$ is on the outside of the torus, $\theta_{mc} = 0.5$ at the inside. With $|B_0| \approx 2.5$ T, the difference between the planar-coil currents (see Tab. 1) results in $\max |B_{1n}|/|B_0| \approx 0.004$ on the boundary. Since W7-X is a left-handed stellarator, $B_{1n} < 0$ at the bottom of the plasma column and $B_{1n} > 0$ at its top, causing an inward shift. This change in the external field retains the five-fold periodicity of the device.

In the right frame of Fig. 2 the free-boundary normal displacement $\vec{\xi} \cdot \nabla s$ is given which describes the inward shift as calculated by the CAS3D code (red). This displacement continuously matches the the external B_{1n} of Fig. 2 (left). The computation was done using 301 radial mesh points and fifteen perturbation harmonics. The CAS3D result compares well to the normal displacement (black) obtained from the difference in the surfaces of two NEMEC runs, i.e. for the basic high-ι and the inward-shifted cases.

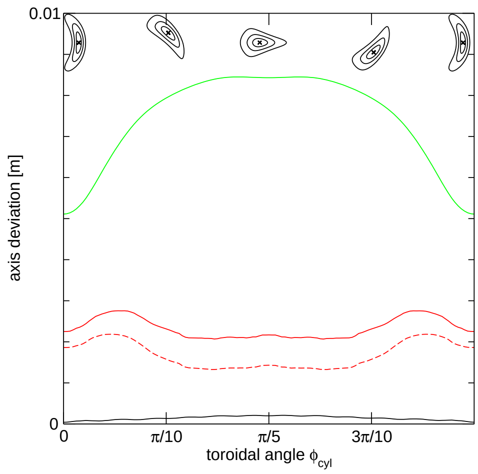

Figure 4: The deviation of the magnetic axis due to an off-balance of planar-coil currents: axis deviation from inward shift (green); precision of CAS3D results (red) from the comparison to the inward-shifted vacuum field: 201 radial grid points (solid line), 301 radial grid points (dashed); precision of NEMEC reconstruction of the basic high-ι W7-X (black).

As a new feature the CAS3D code now calculates the unperturbed and perturbed magnetic field data on a cylindrical spatial grid for subsequent use by a field line tracer. In Fig. 3, the inward shift of the plasma column is illustrated by the magnetic axis and three field-lines on the cross-section at a quarter of a field period (left frame) and half of a period (right frame). The unperturbed (black) and perturbed (red) vacuum fields are compared with the perturbed field (green) resulting from CAS3D in its perturbed-equilibrium version. The perturbed surfaces from CAS3D agree well with the perturbed surfaces from the inward-shifted vacuum field. The same applies to the magnetic axis, as may be seen in Fig. 4, too. The maximum deviation of the magnetic axis from its unperturbed position is ≈ 8.5 mm and occurs in the triangular cross-section. In this cross-section the CAS3D calculation determines the axis with an error of ≈ 1.4 mm. Because of the indentation, the ratio of error to deviation is most unfavorable in the bean-shaped cross-section, and is approximately equal to $1.8/5.1$.

4 Summary

The perturbed-equilibrium method as implemented in the CAS3D code was successfully applied for studying the impact of an external field on the W7-X high-ι variant with $\iota \approx 1$ near the magnetic axis and $\iota \approx 5/4$ near the plasma edge. As a new feature the code can now store the perturbed magnetic field on a cylindrical-coordinates grid for subsequent field-line tracing. The benchmark was conducted at zero plasma-β and used vacuum fields for comparison. Future extensions of this work comprise the study of finite plasma-β and perturbations which destroy the five-fold symmetry of W7-X plasmas.

References

[1] NÜHRENBERG, J. et al., Trans. Fusion Technol. **27** (2009) 106.

[2] WEGENER, L., Fus. Engineering Design **84** (2009) 106.

[3] BOOZER, A. H., Perturbed plasma equilibria, Phys. Plasmas **6** (1999) 831.

[4] HIRSHMAN, S. P. et al., Three-dimensional free boundary calculations using a spectral Green's function method, Comput. Phys. Commun. **43** (1986) 143.

[5] DREVLAK, M. et al., PIES free boundary stellarator equilibria with improved initial conditions, Nucl. Fusion **45** (2005) 731.

[6] NÜHRENBERG, C. et al., Magnetic-surface quality in nonaxisymmetric plasma equilibria, Phys. Rev. Lett. **102** (2009) 235001.